

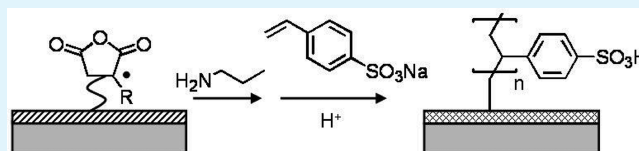
# Pulsed Plasmachemical Deposition of Highly Proton Conducting Composite Sulfonic Acid–Carboxylic Acid Films

T. J. Wood and J. P. S. Badyal\*

Department of Chemistry, Science Laboratories, Durham University, Durham DH1 3LE, England, United Kingdom

**ABSTRACT:** Graft polymerization of sulfonic acid monomers onto structurally well-defined pulsed plasma poly(maleic anhydride) layers yields a composite carboxylic acid–sulfonic acid network. These bifunctional films are shown to exhibit high proton conductivity ( $125 \text{ mS cm}^{-1}$ ) as well as good stability in water.

**KEYWORDS:** proton conduction, composite layer, thin film, plasma deposition, polymer brush, ion exchange



## 1. INTRODUCTION

There exists a strong demand for cost-effective and high-performance proton exchange/ion conducting membranes for applications such as fuel cells,<sup>1,2</sup> lithium ion batteries,<sup>3,4</sup> gas sensors,<sup>5</sup> ion exchange resins,<sup>6</sup> electro dialysis,<sup>7</sup> and ultra-filtration.<sup>8</sup> Nafion is the current industry benchmark for proton conducting membranes. It consists of perfluorosulfonic acid groups pendant off a poly(tetrafluoroethylene) backbone, and yields a proton conductivity of around  $80\text{--}90 \text{ mS cm}^{-1}$  at room temperature when fully hydrated.<sup>9–12</sup> The inherently high costs and environmental impact of Nafion proton exchange membrane manufacture means that there is an impetus for the development of alternative highly proton conducting membranes that are stable in water and easy to manufacture.<sup>13</sup> Some potential candidates have included poly(styrene),<sup>14,15</sup> poly(imide),<sup>16</sup> poly(aryl ether),<sup>17,18</sup> or poly(phosphazene)<sup>19,20</sup> hydrophobic backbones, which are either copolymerized with a hydrophilic acid-containing moiety,<sup>16,17</sup> sulfonated post polymerization,<sup>21,22</sup> or have hydrophilic acid-containing polymer chains grafted onto the hydrophobic backbone.<sup>23–25</sup> Amongst these polymer backbone functionalization methods, grafting is particularly attractive because it can yield higher proton conductivity values.<sup>23,24</sup>

Such graft polymerization techniques can be divided into either graft-from methods, where free radical creation within the polymer backbone is induced by radiation followed by growth of acid-containing polymer;<sup>26–28</sup> or graft-to approaches, where polymer brushes are synthesized beforehand and then attached to the polymer backbone via a reactive moiety (e.g., a double bond).<sup>23</sup> However, both ways suffer from various shortfalls: radiation-induced grafting-from can cause damage to the polymer backbone,<sup>26</sup> whereas graft-to requires multistep syntheses and involves prolonged reaction times.<sup>23</sup>

In contrast to the aforementioned complex membrane fabrication techniques, plasma polymerization is a much more straightforward and solventless methodology.<sup>29</sup> Previous plasma-deposited proton exchange membranes have suffered from low proton conductivity<sup>30–39</sup> and susceptibility towards cracking when hydrated.<sup>40,41</sup> The present study utilizes a

variant of conventional plasmachemical deposition, which entails modulating the electrical discharge in order to trigger monomer activation and reactive site generation at the surface (via VUV irradiation, ion, or electron bombardment) during each short duty cycle on-period (microseconds), followed by conventional carbon–carbon double bond polymerization of the precursor molecules during the extended duty cycle off-periods (milliseconds).<sup>42</sup> This approach leads to high levels of structural retention within the deposited layer, where examples of functionalities include: carboxylic acid,<sup>43</sup> amine,<sup>44</sup> cyano,<sup>45</sup> epoxide,<sup>46</sup> hydroxyl,<sup>47</sup> halide,<sup>48</sup> thiol,<sup>49</sup> furfuryl,<sup>50</sup> perfluoroalkyl,<sup>51</sup> perfluoromethylene,<sup>52</sup> and trifluoromethyl<sup>53</sup> groups. Moreover, it has been shown that by careful tuning of the pulsed plasma duty cycle, free radicals may be trapped within the deposited films and subsequently utilized to initiate conventional graft-from polymerization.<sup>54</sup>

In this investigation, we prepare anhydride-containing films by pulsed plasmachemical deposition, which are then activated by reaction with propylamine (aminolysis). This derivatization with propylamine leads to swelling of the anhydride layers, which provides greater access to subsurface free radicals trapped within the plasmachemical films.<sup>54</sup> These free radicals are then able to act as initiator sites for graft polymerization of sodium 4-styrene sulfonate (which is easily converted into sulfonic acid groups), Scheme 1.

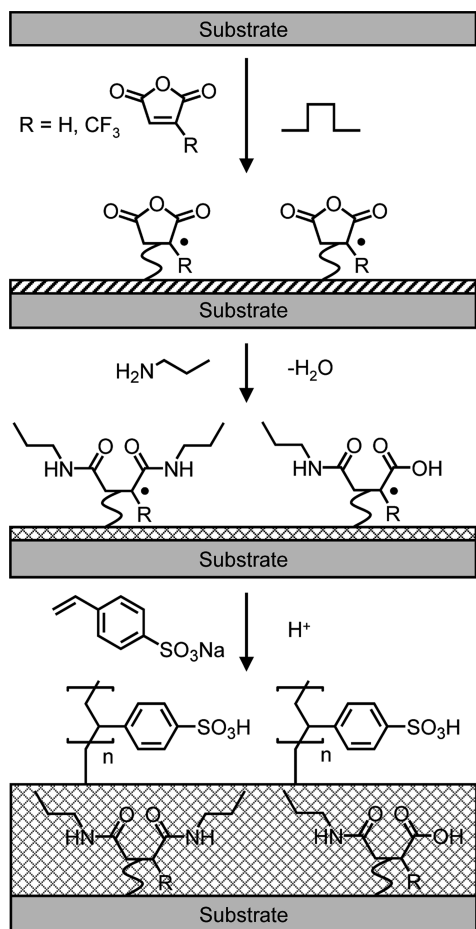
Although surface grafted films proton conducting films have been reported previously,<sup>55–59</sup> this is the first time that carboxylic acid-containing polymer backbone films with intrinsic proton conductivity have been combined with grafted sulfonic acid-containing polymer brushes to yield composite structures with high proton conductivity. Furthermore, the measured proton conductivities are greater than or equal to Nafion, and these layers exhibit good stability in water.

**Received:** December 22, 2011

**Accepted:** February 24, 2012

**Published:** March 12, 2012

**Scheme 1. Pulsed Plasmachemical Deposition of Free Radical Containing Anhydride Films Followed by Activation with Propylamine Vapour and Subsequent Graft-from Polymerization of Poly(sodium 4-styrenesulfonate)**



## 2. EXPERIMENTAL SECTION

### 2.1. Preparation of Poly(4-styrenesulfonic acid) Graft Layers.

Plasma deposition was carried out in an electrodeless cylindrical glass reactor (volume of 480 cm<sup>3</sup>, base pressure of  $3 \times 10^{-3}$  mbar, and with a leak rate better than  $2 \times 10^{-9}$  mol s<sup>-1</sup>) surrounded by a copper coil (4 mm diameter, 10 turns), and enclosed in a Faraday cage. The chamber was pumped down using a 30 L min<sup>-1</sup> rotary pump attached to a liquid nitrogen cold trap; a Pirani gauge was used to monitor system pressure. The output impedance of a 13.56 MHz radio frequency (rf) power supply was matched to the partially ionized gas load via an L-C circuit. Prior to each deposition, the reactor was scrubbed using detergent, rinsed in propan-2-ol, and dried in an oven. A continuous wave air plasma was then run at 0.2 mbar pressure and 40 W power for 30 min in order to remove any remaining trace contaminants from the chamber walls. Substrates used for coating were silicon (100) wafer pieces (Silicon Valley Microelectronics Inc.), polypropylene sheet (Lawson Mardon Ltd.) each with two evaporated gold electrodes (5 mm length and 1.5 mm separation) for proton conductivity testing. Borosilicate glass slides (VWR Ltd.) were used for radical density quantification measurements. Maleic anhydride briquettes (+99%, Aldrich Ltd., ground into a fine powder) and trifluoromethyl-maleic anhydride (+97%, Apollo Scientific Ltd.) were loaded into separate sealable glass tubes and degassed using multiple freeze-pump-thaw cycles. Precursor vapour was allowed to purge the reactor for 5 min at a pressure of 0.2 mbar prior to electrical discharge ignition. Pulsed plasma deposition utilized an optimal duty cycle of 20  $\mu$ s on-period and 1200  $\mu$ s off-period in conjunction with a peak power of 5 W.<sup>42</sup> Upon plasma extinction, the precursor vapor continued to

pass through the system for a further 3 min, and then the chamber was evacuated back down to base pressure.

The plasma-deposited anhydride-containing films were subsequently derivatized by exposure to propylamine (Aldrich Ltd.) vapour at a pressure of 200 mbar for 30 min, followed by evacuation of the system back down to base pressure.

Next, the propylamine-derivatized anhydride-containing films were placed into a sealable glass tube together with 18 wt % sodium 4-styrenesulfonate (Aldrich Ltd.) solution in water. This mixture was subjected to several freeze-pump-thaw cycles until fully degassed, whereupon the tube was placed into an oil bath at 50 °C to initiate graft-from polymerization. Upon completion of reaction, the substrates were washed in high purity water (pH 7.0) and aqueous acetic acid (Fisher Scientific Ltd.) solution (pH 3.7) in order to effect ion exchange between Na<sup>+</sup> and H<sup>+</sup>. Finally, the samples were allowed to dry in air at room temperature.

**2.2. Film Characterization.** Surface elemental compositions were determined by X-ray photoelectron spectroscopy (XPS) using a VG ESCALAB II electron spectrometer equipped with a non-monochromated Mg K $\alpha$  X-ray source (1253.6 eV) and a concentric hemispherical analyser. Photoemitted electrons were collected at a take-off angle of 20° from the substrate normal, with electron detection in the constant analyser energy mode (CAE, pass energy = 20 eV). Experimentally determined instrument sensitivity factors were taken as C(1s):O(1s):F(1s):N(1s):Na(1s):S(2p) equals 1.00:0.34:0.26:0.66:0.05:0.55. All binding energies were referenced to the C(1s) hydrocarbon peak at 285.0 eV. A linear background was subtracted from core level spectra and then fitted using Gaussian peak shapes with a constant full-width-half-maximum (fwhm).<sup>60</sup>

Infrared spectra were acquired using a FTIR spectrometer (Perkin-Elmer Spectrum One) fitted with a liquid nitrogen cooled MCT detector operating at 4 cm<sup>-1</sup> resolution across the 700–4000 cm<sup>-1</sup> range. The instrument included a variable angle reflection-absorption accessory (Specac Ltd) set to a grazing angle of 66° for silicon wafer substrates and adjusted for p-polarization.

The concentration of radical sites present in the films was determined using 2,2-diphenyl-1-picrylhydrazyl (DPPH, 95%, Aldrich Ltd).<sup>61</sup> A borosilicate glass coverslip slide coated with the plasmachemical films was placed into a glass tube containing  $1 \times 10^{-4}$  mol dm<sup>-3</sup> solution of DPPH in toluene (which had been thoroughly degassed using multiple freeze-pump-thaw cycles). The tube was then heated to 50 °C for 30 min. The DPPH molecules consumed by surface radicals were quantified using a spectrophotometer (Philips Scientific Ltd, PU 8625) by measuring the difference in absorbance at 520 nm between the starting solution and following immersion of each coated sample.

Film thicknesses were measured using a spectrophotometer (nk6000, Aquila Instruments Ltd.). Transmittance-reflectance curves (350–1000 nm wavelength range) were acquired for each sample and fitted to a Cauchy material model using a modified Levenberg-Marquardt algorithm.<sup>62</sup>

Proton conductivity values were obtained by undertaking impedance measurements across the 10 Hz–13 MHz frequency range using an LF impedance analyser (Hewlett-Packard, 4192A) for coated polypropylene substrates whilst submerged in ultra high purity water at 20 °C. The low frequency 45° line in the acquired impedance plots was assigned to the Warburg diffusion impedance, and a high frequency arc was fitted in order to extract the resistance of the plasmachemical deposited membrane layer from its intercept of the real axis at the lower frequency end.<sup>12</sup> The formula  $\sigma = l/R_s A$  was used to calculate proton conductivity, where  $\sigma$  is the membrane conductivity,  $R_s$  is the bulk membrane resistance,  $l$  is the length of the electrodes, and  $A$  is the cross-sectional area of the film.<sup>63</sup> Controls showed that uncoated polypropylene with and without the presence of water gave rise to no conductivity (either ionic or electronic). Further proton conductivity tests were carried out at 20 °C in the absence of immersion in water, but in the presence of a relative humidity of 97% by using a saturated potassium sulfate (+99%, Sigma-Aldrich Ltd.) solution in water.<sup>64</sup>

Ion exchange capacities were calculated by taking the difference in measured sodium XPS content between washing in acetic acid and after washing in sodium chloride (+99.5%, Sigma-Aldrich Ltd.) aqueous solution. This gave an ion exchange capacity of 5.4 mequiv  $g^{-1}$  for the poly(sodium 4-styrenesulfonate) films (regardless of precursor layer).

Accelerated oxidation stability tests were carried out by immersing the films into an aqueous solution of 12 mM hydrogen peroxide (diluted from 35 wt % hydrogen peroxide in water, Sigma-Aldrich Ltd) which contained 40 ppm  $Fe^{2+}$  (iron(II) sulfate, 99%, BDH Chemicals Ltd), and placing in an oven at 65 °C for 1 h.<sup>65,66</sup> No degradation was observed, which is consistent with the use of poly(sodium 4-styrenesulfonate) for fuel cell membranes.<sup>67</sup>

### 3. RESULTS

**3.1. Poly(4-sodium styrenesulfonate) Grafted onto Plasma-Deposited Anhydride Layers.** Pulsed plasma-deposited poly(maleic anhydride) layers display a distinctive XPS C(1s) component peak at 288.9 eV (O-C=O) corresponding to anhydride carbon centers,<sup>42</sup> Figure 1.

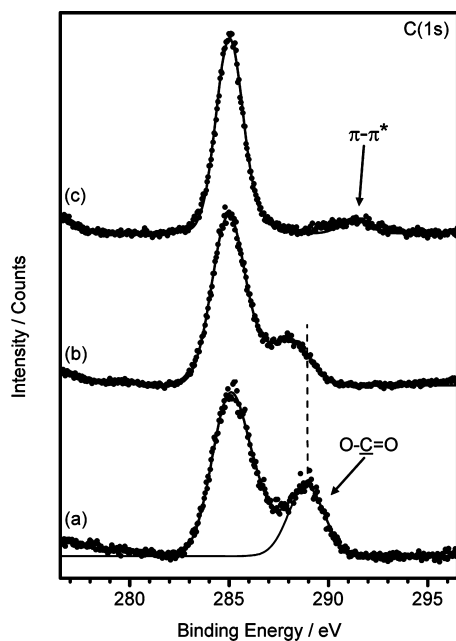


**Figure 1.** C(1s) XPS spectra for: (a) pulsed plasma-deposited poly(maleic anhydride); (b) propylamine-derivatized pulsed plasma-deposited poly(maleic anhydride); and (c) poly(sodium 4-styrenesulfonate) grafted onto propylamine-derivatized pulsed plasma poly(maleic anhydride).

Following reaction with propylamine, this feature shifts to 288.0 eV (N-C=O), which is consistent with aminolysis having taken place.<sup>68</sup> This is accompanied by an increase in the hydrocarbon (C-H) component peak at 285.0 eV attributable to the alkyl chain of propylamine. Subsequent graft polymerization of sodium 4-styrenesulfonate resulted in the loss of the anhydride/amide shoulder peak to leave the predominant hydrocarbon (C-H) feature. This is consistent with there being complete coverage by poly(sodium 4-styrenesulfonate) of the poly(maleic anhydride) initiator layer. A low intensity  $\pi-\pi^*$  shake-up feature at 291.0 eV characteristic of the phenyl centers is also observed.<sup>68</sup>

A similar series of reactions was shown to occur for pulsed plasma-deposited poly(trifluoromethyl-maleic anhydride) layers, which initially display the distinctive anhydride

component peak at 288.9 eV (O-C=O) as well as a feature at 292.5 eV (CF<sub>3</sub>) characteristic of trifluoromethyl centers,<sup>69</sup> Figure 2. This trifluoromethyl peak remains following

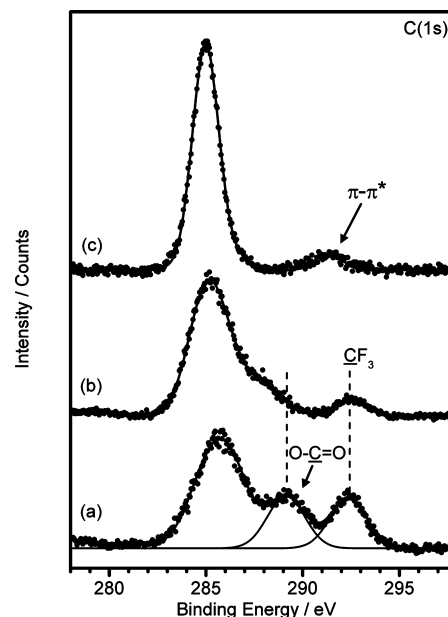


**Figure 2.** C(1s) XPS spectra for: (a) pulsed plasma-deposited poly(trifluoromethyl-maleic anhydride); (b) propylamine-derivatized pulsed plasma-deposited poly(trifluoromethyl-maleic anhydride); and (c) poly(sodium 4-styrenesulfonate) grafted onto propylamine-derivatized pulsed plasma poly(trifluoromethyl-maleic anhydride).

aminolysis, but disappears upon coverage by the grafted poly(4-styrenesulfonate).

For both types of anhydride initiator layer, the absence of any Si(2p) XPS signal from the underlying silicon substrate confirmed pin-hole free coverage. For the propylamine-derivatized films, carbon, oxygen and nitrogen signals were detected (along with fluorine in the case of pulsed plasma-deposited poly(trifluoromethyl-maleic anhydride) confirming reaction of the propylamine with the anhydride functionalities, Table 1. The N:O ratio for the propylamine-derivatized pulsed plasma-deposited poly(maleic anhydride) films was 1.0:2.4, whereas a much higher ratio of 1.0:1.1 was measured for the propylamine-derivatized pulsed plasma-deposited poly(trifluoromethyl-maleic anhydride) layers. This is indicative of the anhydride rings being more susceptible towards complete aminolysis for the latter and is supported by the accompanying N(1s) XPS region, which shows a single-component peak at 399.8 eV (corresponding to amide O=C-N(H)-C group formation<sup>68</sup>), whereas in the case of pulsed plasma-deposited poly(maleic anhydride), there is an extra smaller peak at 401.6 eV (assigned to C-NH<sub>3</sub><sup>+</sup> centers and hence only partial aminolysis<sup>68</sup>), Figure 3 and Scheme 1. Elemental XPS concentrations for subsequent thermally grafted poly(sodium 4-styrenesulfonate) films show good agreement with the predicted theoretical polymer structure, Table 1. The cationic sodium content is measured to be less as a consequence of some ion exchange with H<sup>+</sup> having taken place during the cleaning step with water and aqueous acetic acid following graft polymerization. This was proven by deliberately soaking in pH 3.7 acetic acid solution, which gave rise to the complete disappearance of the sodium XPS signal, whereas other

Table 1. XPS Elemental Compositions

layer	% C	% O	% F	% N	% Na	% S
pulsed plasma poly(maleic anhydride)	67 ± 1	33 ± 1				
pulsed plasma poly(trifluoromethyl-maleic anhydride)	52 ± 1	15 ± 1	33 ± 1			
propylamine-derivatized pulsed plasma poly(maleic anhydride)	69 ± 1	22 ± 1		9 ± 1		
propylamine-derivatized pulsed plasma poly(trifluoromethyl-maleic anhydride)	63 ± 1	10 ± 1	19 ± 1	9 ± 1		
theoretical poly(sodium 4-styrenesulfonate)	62	23			8	8
poly(sodium 4-styrenesulfonate) thermally grafted onto propylamine-derivatized pulsed plasma poly(maleic anhydride)	67 ± 1	22 ± 1			3 ± 1	9 ± 1
poly(sodium 4-styrenesulfonate) thermally grafted onto propylamine-derivatized pulsed plasma poly(trifluoromethyl-maleic anhydride)	66 ± 1	22 ± 1			4 ± 1	9 ± 1

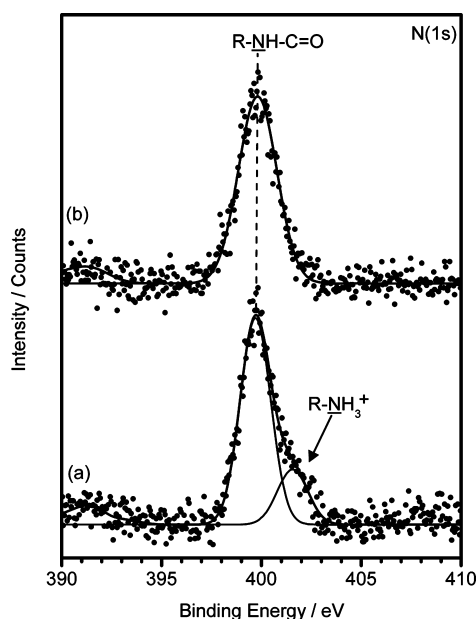


**Figure 3.** N(1s) XPS spectra following propylamine derivatization of: (a) pulsed plasma-deposited poly(maleic anhydride); and (b) pulsed plasma-deposited poly(trifluoromethyl-maleic anhydride).

elements remained, thus confirming that ion exchange of  $\text{Na}^+$  for  $\text{H}^+$  can take place.

Infrared spectra for the pulsed plasma-deposited poly(maleic anhydride) films show fingerprint anhydride symmetrical ( $1870\text{ cm}^{-1}$ ) and antisymmetrical ( $1800\text{ cm}^{-1}$ )  $\text{C}=\text{O}$  stretches,<sup>42</sup> Figure 4. Propylamine derivatization causes attenuation of the anhydride peak ( $1800\text{ cm}^{-1}$ ) with the concurrent appearance of a carboxylic acid antisymmetrical  $\text{C}=\text{O}$  stretch ( $1711\text{ cm}^{-1}$ ), amide  $\text{C}=\text{O}$  stretch ( $1656\text{ cm}^{-1}$ , amide I), and amide  $\text{C}-\text{N}-\text{H}$  stretch bend ( $1577\text{ cm}^{-1}$ , amide II). Alkyl group features are also evident with  $\text{CH}_3$  antisymmetrical stretch ( $2966\text{ cm}^{-1}$ ),  $\text{CH}_2$  antisymmetrical stretch ( $2936\text{ cm}^{-1}$ ), and  $\text{CH}_3$  symmetrical stretch ( $2874\text{ cm}^{-1}$ ), along with a broad band corresponding to the amide  $\text{N}-\text{H}$  stretch ( $3250\text{ cm}^{-1}$ ). Subsequent graft polymerization of sodium 4-styrenesulfonate gave rise to the appearance of the  $\text{SO}_3$  symmetrical stretch ( $1045\text{ cm}^{-1}$ ), together with the phenyl ring in-plane skeleton vibration ( $1134\text{ cm}^{-1}$ ), and in-plane bending vibration ( $1012\text{ cm}^{-1}$ ), Figure 4.<sup>70</sup>

In the case of pulsed plasma-deposited poly(trifluoromethyl-maleic anhydride) films, the infrared spectra display similar changes, with there being initially characteristic anhydride  $\text{C}=\text{O}$  symmetrical ( $1880\text{ cm}^{-1}$ ) and antisymmetrical ( $1809\text{ cm}^{-1}$ ) peaks, Figure 5. These completely disappear upon propylamine derivatization, thereby confirming complete reaction through-

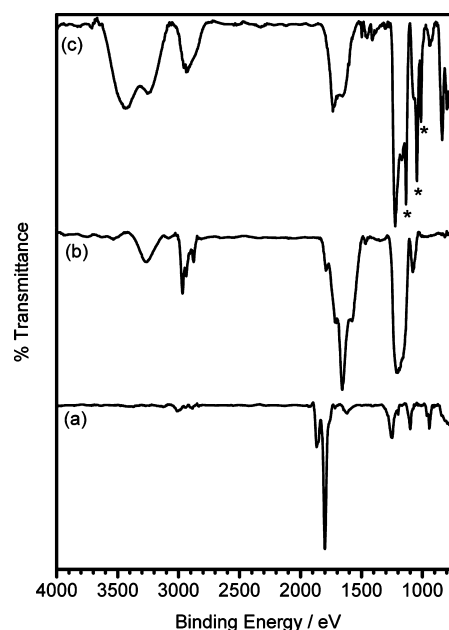


**Figure 4.** Infrared spectra of: (a) pulsed plasma-deposited poly(maleic anhydride); (b) propylamine-derivatized pulsed plasma-deposited poly(maleic anhydride); and (c) poly(sodium 4-styrenesulfonate) layer grafted from propylamine-derivatized pulsed plasma-deposited poly(maleic anhydride). \* Denotes characteristic benzenesulfonate peaks.

out the plasma-deposited layer, whereas graft polymerization of sodium 4-styrenesulfonate similarly gave rise to the appearance of the characteristic  $\text{SO}_3$  symmetrical stretch ( $1045\text{ cm}^{-1}$ ), along with the phenyl ring in-plane skeleton vibration ( $1134\text{ cm}^{-1}$ ), and in-plane bending vibration ( $1012\text{ cm}^{-1}$ ), Figure 5.

Free radical density assays show that the radical density for the pulsed plasma poly(trifluoromethyl-maleic anhydride) is tenfold greater compared to pulsed plasma poly(maleic anhydride), which can be attributed to the stabilizing effect of the electron withdrawing trifluoromethyl group, Table 2. Derivatization by propylamine gives rise to a much higher density of accessible surface radicals for both types of anhydride-containing layer, whereas the number of radicals measured was below the detection limit after the poly(sodium 4-styrenesulfonate) grafting step.

Film thickness measurements for both types of plasma-deposited anhydride containing layers showed approximately 100% swelling upon propylamine derivatization, which can be attributed to the aminolysis reaction,<sup>54</sup> Table 2. Subsequent graft polymerization of poly(sodium 4-styrenesulfonate) films was found to be more rapid for the propylamine-derivatized plasma-deposited poly(trifluoromethyl-maleic anhydride) films

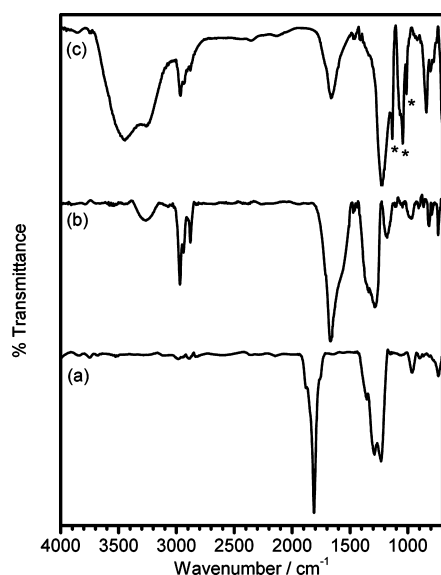


**Figure 5.** Infrared spectra of: (a) pulsed plasma-deposited poly(trifluoromethyl-maleic anhydride); (b) propylamine-derivatized pulsed plasma-deposited poly(trifluoromethyl-maleic anhydride); and (c) poly(sodium 4-styrenesulfonate) layer grafted from propylamine-derivatized pulsed plasma-deposited poly(trifluoromethyl-maleic anhydride). \* Denotes characteristic benzenesulfonate bands.

compared to their maleic anhydride analogue, which is consistent with there being a higher concentration of radicals. Film thicknesses did not significantly increase beyond 1 h grafting time, which can be attributed to termination reactions taking place under aqueous conditions.<sup>71</sup>

Water uptake is significant for pulsed plasma-deposited layers because of the high inherent content of hydrolysable anhydride groups, Table 2. This decreases in the case of derivatization with propylamine, which can be attributed to the increase in weight associated with the additional propyl alkyl chain. Subsequent poly(sodium 4-styrenesulfonate) grafting from these films gives rise to an increase in water uptake due to the inherent hydrophilicity of the grown polymer brushes.

**3.2. Proton Conductivity.** Proton conductivity values of  $50 \pm 5 \text{ mS cm}^{-1}$  and  $90 \pm 5 \text{ mS cm}^{-1}$  were measured for pulsed plasma-deposited poly(maleic anhydride) and poly(trifluoromethyl-maleic anhydride) films respectively upon immersion in water, Figure 6. These proton conductivities were drastically reduced for both films upon aminolysis (10 and  $20 \text{ mS cm}^{-1}$  respectively), which can be attributed to the loss of free carboxylic acid centers due to reaction taking place with propylamine. Subsequent thermal graft polymerization of sodium 4-styrenesulfonate gave rise to a significant increase in proton conductivity exceeding the values for the parent films

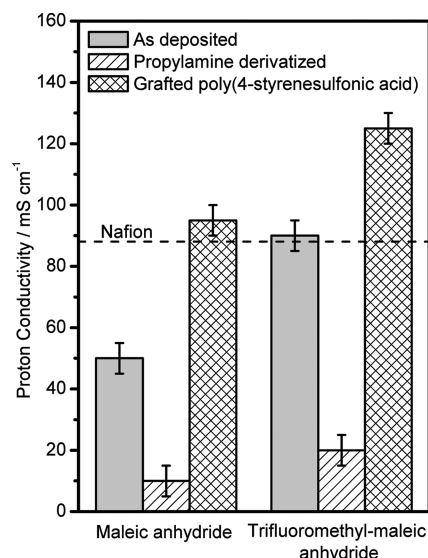


**Figure 6.** Proton conductivity upon immersion in water at  $20^\circ\text{C}$  for pulsed plasma-deposited anhydride films: as deposited; after reaction with propylamine; and subsequent grafting of poly(sodium 4-styrenesulfonate) followed by proton exchange. Note that no enhanced proton conductivity behaviour was observed following graft polymerization of poly(sodium 4-styrenesulfonate) in the absence of propylamine derivatization.

(95 and  $125 \text{ mS cm}^{-1}$ , respectively), Figures 6 and 7. The higher proton conductivity of the poly(4-styrenesulfonic acid)

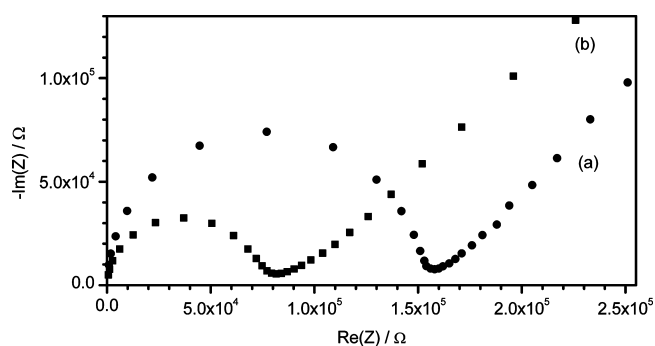


**Figure 7.** Typical impedance plots for poly(sodium 4-styrenesulfonate) thermally grafted onto propylamine-derivatized: (a) pulsed plasma poly(maleic anhydride) and (b) pulsed plasma poly(trifluoromethyl-maleic anhydride).

films grafted from the propylamine-derivatized pulsed plasma-deposited poly(trifluoromethyl-maleic anhydride) layers can be attributed to the more extensive grafting, and therefore greater

**Table 2.** Film Thickness, Growth Rate, Radical Density, and Water Uptake

film	thickness (nm)	growth rate (nm min <sup>-1</sup> )	radical density ( $\times 10^{-9} \text{ mol cm}^{-2}$ )	water uptake (wt %)
pulsed plasma poly(maleic anhydride)	$98 \pm 4$	$3 \pm 1$	$2.6 \pm 0.2$	$167 \pm 7$
pulsed plasma poly(trifluoromethyl-maleic anhydride)	$101 \pm 5$	$6 \pm 1$	$31 \pm 2$	$143 \pm 3$
propylamine-derivatized pulsed plasma poly(maleic anhydride)	$197 \pm 7$		$37 \pm 2$	$120 \pm 10$
propylamine-derivatized pulsed plasma poly(trifluoromethyl-maleic anhydride)	$211 \pm 8$		$52 \pm 4$	$90 \pm 10$
poly(sodium 4-styrenesulfonate) thermally grafted onto propylamine-derivatized pulsed plasma poly(maleic anhydride), 1 h	$248 \pm 9$	$0.8 \pm 0.2$	$0.0 \pm 0.1$	$140 \pm 10$
poly(sodium 4-styrenesulfonate) thermally grafted onto propylamine-derivatized pulsed plasma poly(trifluoromethyl-maleic anhydride), 1 h	$292 \pm 9$	$1.3 \pm 0.2$	$0.0 \pm 0.1$	$120 \pm 10$

density of sulfonic acid groups (which are known to underpin proton conductivity). Control samples in the absence of propylamine derivatization did not show this enhanced proton conductivity behaviour following graft polymerization of poly(sodium 4-styrenesulfonate). Furthermore, no cracking in the films upon hydration was observed.

For the case of 97% relative humidity (rather than immersion in water), very low proton conductivities were measured for the pulsed plasma poly(maleic anhydride) and poly(trifluoromethyl-maleic anhydride) layers and also for their propylamine-derivatized counterparts. Whereas, following subsequent poly(4-styrenesulfonic acid) brush grafting, the poly(maleic anhydride) and poly(trifluoromethyl-maleic anhydride) based layers displayed values of  $70 \pm 10$  mS cm<sup>-1</sup> and  $110 \pm 10$  mS cm<sup>-1</sup>, respectively.

#### 4. DISCUSSION

Pulsed plasma deposition of anhydride-containing films effectively provides a single-step process for preparing proton exchange membranes at ambient temperatures. This is particularly well-suited for the fabrication of micro fuel cells.<sup>72</sup> It is envisaged that film thickness can be controlled by either varying the duration of deposition or by utilising an atomiser for faster rates.<sup>73</sup> Upon immersion in water, the inherent high density of carboxylic acid functionalities gives rise to proton conductivity. Propylamine derivatization leads to a drop in proton conduction, which can be explained on the basis of loss of proton conducting carboxylic acid centers because of their consumption in the aminolysis reaction, Scheme 1. Grafting of poly(sodium 4-styrenesulfonate) layers from these aminolyzed carboxylic anhydride membranes leads to a large enhancement in conductivity yielding 125 mS cm<sup>-1</sup> at room temperature for the trifluoromethyl variant, Figure 6. This compares favorably to the current benchmark standard, Nafion, which has a proton conductivity of 80–90 mS cm<sup>-1</sup> under similar test conditions.<sup>12</sup> The relative humidity (rather than immersion in water) experiments have shown that the carboxylic acid centers need a relatively high level of water content to facilitate proton conductivity, whereas the grafted polymer brush sulfonic acid centers require far less. A similar drop in proton conductivity has previously been reported for Nafion when moving from water immersion to high relative humidity.<sup>74,75</sup>

An estimate can be made of the grafted polymer brush lengths based on the radical density of the layer, the thickness of the grafts, and the density of poly(sodium 4-styrene sulfonate); this gives average values of around 40 monomer units per chain for the poly(sodium 4-styrene sulfonate) graft from propylamine-derivatized poly(maleic anhydride) and 65 units per chain for the poly(sodium 4-styrene sulfonate) from propylamine-derivatized poly(trifluoromethyl-maleic anhydride).

A threefold beneficial effect is observed for the trifluoromethyl group substituted variant of maleic anhydride precursor: firstly it stabilizes anhydride radicals within the electrical discharge<sup>76</sup> (thus enhancing polymer chain growth during the plasma duty cycle off-period, and also increases the density of radicals contained within the film that can act as initiation centers during the subsequent grafting step of sodium 4-styrenesulfonate<sup>77,78</sup>); secondly, its electron-withdrawing effect makes the carboxylic acid group more acidic (therefore higher proton conductivity);<sup>79</sup> and finally, it makes the carbonyl center more susceptible towards nucleophilic attack,<sup>80</sup> thus

maximizing the extent of aminolysis, which helps to enhance the density of radicals contained in the functional layer.<sup>54</sup> Anhydride rings are known to be particularly good at stabilizing radicals because of resonance effects enabled by the cyclic conjugated anhydride structure.<sup>81</sup> The corresponding propylamine-derivatized carboxylic-anhydride films have been shown to be sufficiently robust to allow growth of sulfonic acid-containing polymer brushes as well as being stable afterwards in water. This is in marked contrast with previous plasma-deposited proton exchange membranes, which suffer from a lack of stability upon hydration.<sup>40,41</sup>

The outlined plasmachemical deposition process followed by propylamine derivatization, and the grafting of sulfonic acid containing polymer brushes, is simple, quick to manufacture, and utilizes water as a solvent (minimal environmental impact in marked contrast to Nafion).<sup>82</sup> Additionally, plasmachemical deposition provides a single-step deposition directly onto components (such as platinum loaded carbon black particles for fuel cells), which enables ease of manufacture by avoiding solvent casting techniques, which inherently give rise to lack of conformality.<sup>83</sup>

#### 5. CONCLUSIONS

Pulsed plasmachemical deposition using maleic anhydride precursors yields structurally well-defined thin films. Subsequent aminolysis reaction at the anhydride centers using a spacer molecule causes swelling, which provides access to initiator free radical centers for the grafting of sulfonic-acid containing polymer brushes. The resultant functional layers yield proton conductivity values exceeding or on a par with Nafion. The inherent capability to conformally coat device components with highly proton-conducting membranes offers advantages in terms of lower cost, ease of manufacture, and avoidance of environmentally unfriendly nonaqueous processing.

#### AUTHOR INFORMATION

##### Corresponding Author

\*E-mail: j.p.badyal@durham.ac.uk.

##### Notes

The authors declare no competing financial interest.

#### ACKNOWLEDGMENTS

Professor M. C. Petty and Dr C. Pearson from School of Engineering and Computing Sciences, Durham University, are thanked for their assistance with the proton conduction measurements.

#### REFERENCES

- (1) Service, R. F. *Science* **2002**, 296, 1222.
- (2) *2010 Annual Report*; Hydrogen and Fuel Cell Technical Advisory Committee, U. S. Department of Energy: Washington, D.C., 2011.
- (3) Crittenden, J. C.; White, H. S. *J. Am. Chem. Soc.* **2004**, 132, 4503.
- (4) Kerr, R. L.; Miller, S. A.; Shoemaker, R. K.; Elliott, B. J.; Gin, D. L. *J. Am. Chem. Soc.* **2009**, 131, 15972.
- (5) van der Wal, P. D.; de Rooij, N. F.; Koudelka-Hep, M. *Sens. Actuators, B* **1996**, 35, 119.
- (6) Monterroso, S. C. C.; Carapuça, H. M.; Duarte, A. C. *Talanta* **2005**, 65, 644.
- (7) Okawara, A.; Horie, H.; Miyake, H.; Nishimura, H. *Polymer* **1992**, 33, 1579.
- (8) Yeager, H. L.; Gronowski, A. A. *Membrane Applications. In Ionomers: Synthesis, Structure, Properties, and Applications*; Tant, M. R.,

- Mauritz, K. A., Wilkes, G. L., Eds.; Chapman & Hall: London, U.K., 1997.
- (9) Spry, D. B.; Goun, A.; Glusac, K.; Moilanen, D. E.; Fayer, M. D. *J. Am. Chem. Soc.* **2007**, *129*, 8122.
- (10) Fontanella, J. J.; Wintersgill, M. C.; Chem, R. S.; Wu, Y.; Greenbaum, S. G. *Electrochim. Acta* **1995**, *40*, 2321.
- (11) Mauritz, K. A.; Moore, R. B. *Chem. Rev.* **2004**, *104*, 4535.
- (12) Mikhailenko, S. D.; Guiver, M. D.; Kaliaguine, S. *Solid State Ionics* **2008**, *179*, 619.
- (13) Costamagna, P.; Srinivasan, S. *J. Power Sources* **2001**, *102*, 242.
- (14) Chen, S.; Benziger, J. B.; Bocarsly, A. B.; Zhang, T. *Ind. Eng. Chem. Res.* **2005**, *44*, 7701.
- (15) Bertran, O.; Curc , D.; Torras, J.; Ferreira, C. A.; Alem n, C. *Macromolecules* **2010**, *43*, 10521.
- (16) Asano, N.; Aoki, M.; Suzuki, S.; Miyatake, K.; Uchida, H.; Watanabe, M. *J. Am. Chem. Soc.* **2006**, *128*, 1762.
- (17) Schmeisser, J.; Holdcroft, S.; Yu, J.; Ngo, T.; McLean, G. *Chem. Mater.* **2005**, *17*, 387.
- (18) Miyatake, K.; Chikashige, Y.; Higuchi, E.; Watanabe, M. *J. Am. Chem. Soc.* **2007**, *129*, 3879.
- (19) Allcock, H. R.; Hofmann, M. A.; Ambler, C. M.; Morford, R. V. *Macromolecules* **2002**, *35*, 3484.
- (20) Hofmann, M. A.; Ambler, C. M.; Maher, A. E.; Chalkova, E.; Zhou, X. Y.; Lvov, S. N.; Allcock, H. R. *Macromolecules* **2002**, *35*, 6490.
- (21) Di Vona, M. L.; Sgreccia, E.; Licoccia, S.; Khadhraoui, M.; Denoyel, R.; Knauth, P. *Chem. Mater.* **2008**, *20*, 4327.
- (22) Kim, S. Y.; Park, M. J.; Balsara, N. P.; Jackson, A. *Macromolecules* **2010**, *43*, 8128.
- (23) Ding, J.; Chuy, C.; Holdcroft, S. *Macromolecules* **2002**, *35*, 1348.
- (24) Tsang, E. M. W.; Zhang, Z.; Shi, Z.; Soboleva, T.; Holdcroft, S. *J. Am. Chem. Soc.* **2007**, *129*, 15106.
- (25) Li, N.; Wang, C.; Lee, S. Y.; Park, C. H.; Lee, Y. M.; Guiver, M. D. *Angew. Chem., Int. Ed.* **2011**, *50*, 9158.
- (26) Gupta, B.; Scherer, G. G. *J. Appl. Polym. Sci.* **1993**, *50*, 2129.
- (27) Yamaki, T.; Asano, M.; Maekawa, Y.; Morita, Y.; Suwa, T.; Chen, J.; Tsubokawa, N.; Kobayashi, K.; Kubota, H.; Yoshida, M. *Radiat. Phys. Chem.* **2003**, *67*, 403.
- (28) Holmberg, S.; Holmlund, P.; Nicolas, R.; Wilen, C.; Kallio, T.; Sundholm, G.; Sundholm, F. *Macromolecules* **2004**, *37*, 9909.
- (29) Yasuda, H. *Plasma Polymerization*; Academic Press: New York, 1985.
- (30) Inagaki, N.; Tasaka, S.; Horikawa, Y. *J. Polym. Sci., Part A: Polym. Chem.* **1989**, *27*, 3495.
- (31) Inagaki, N.; Tasaka, S.; Kurita, T. *Polym. Bull.* **1989**, *22*, 15.
- (32) Ogumi, Z.; Uchimoto, Y.; Takehara, Z. *J. Electrochem. Soc.* **1990**, *137*, 3319.
- (33) Ogumi, Z.; Uchimoto, Y.; Yasuda, K.; Takehara, Z. *Chem. Lett.* **1990**, 953.
- (34) Inagaki, N.; Tasaka, S.; Chengfei, Z. *Polym. Bull.* **1991**, *26*, 187.
- (35) Brumlik, C. J.; Parthasarathy, A.; Chen, W. J.; Martin, C. R. *J. Electrochem. Soc.* **1994**, *141*, 2273.
- (36) Danilich, M. J.; Gervasio, D.; Burton, D. J.; Marchant, R. E. *Macromolecules* **1995**, *28*, 5567.
- (37) Finsterwalder, F.; Hambitzer, G. *J. Membr. Sci.* **2001**, *185*, 105.
- (38) Mahdjoub, H.; Rouldes, S.; Sibat, P.; Pradeilles, N.; Durand, J.; Pourcelly, G. *Fuel Cells* **2005**, *5*, 277.
- (39) Rouldes, S.; Topala, I.; Mahdjoub, H.; Rouessac, V.; Sibat, P.; Durand, J. *J. Power Sources* **2006**, *158*, 1270.
- (40) Thery, J.; Martin, S.; Fauchoux, V.; Le Van Jodin, L.; Truffier-Boutry, D.; Martinent, A.; Laurent, J. Y. *J. Power Sources* **2010**, *195*, 5573.
- (41) Jiang, Z.; Jiang, Z.; Meng, Y. *J. Membr. Sci.* **2011**, *372*, 303.
- (42) Ryan, M. E.; Hynes, A. M.; Badyal, J. P. S. *Chem. Mater.* **1996**, *8*, 37.
- (43) Hutton, S. J.; Crowther, J. M.; Badyal, J. P. S. *Chem. Mater.* **2000**, *12*, 2282.
- (44) Harris, L. G.; Schofield, W. C. E.; Doores, K. J.; Davis, B. G.; Badyal, J. P. S. *J. Am. Chem. Soc.* **2009**, *131*, 7755.
- (45) Tarducci, C.; Schofield, W. C. E.; Brewer, S. A.; Willis, C.; Badyal, J. P. S. *Chem. Mater.* **2001**, *13*, 1800.
- (46) Tarducci, C.; Kimmond, E. J.; Brewer, S. A.; Willis, C.; Badyal, J. P. S. *Chem. Mater.* **2000**, *12*, 1884.
- (47) Tarducci, C.; Schofield, W. C. E.; Brewer, S. A.; Willis, C.; Badyal, J. P. S. *Chem. Mater.* **2002**, *14*, 2541.
- (48) Teare, D. O. H.; Barwick, D. C.; Schofield, W. C. E.; Garrod, R. P.; Ward, L. J.; Badyal, J. P. S. *Langmuir* **2005**, *21*, 11425.
- (49) Schofield, W. C. E.; McGettrick, J.; Bradley, T. J.; Przyborski, S.; Badyal, J. P. S. *J. Am. Chem. Soc.* **2006**, *128*, 2280.
- (50) Tarducci, C.; Brewer, S. A.; Willis, C.; Badyal, J. P. S. *Chem. Commun.* **2005**, 406.
- (51) Coulson, S. R.; Woodward, I. S.; Brewer, S. A.; Willis, C.; Badyal, J. P. S. *Chem. Mater.* **2000**, *12*, 2031.
- (52) Limb, S. J.; Gleason, K. K.; Edell, D. J.; Gleason, E. F. *J. Vac. Sci. Technol.* **1997**, *A15*, 1814.
- (53) Wang, J. H.; Chen, J. J.; Timmons, R. B. *Chem. Mater.* **1996**, *8*, 2212.
- (54) Teare, D. O. H.; Schofield, W. C. E.; Garrod, R. P.; Badyal, J. P. S. *Langmuir* **2005**, *21*, 10818.
- (55) Chen, H.; Palmese, G. R.; Elabd, Y. A. *Chem. Mater.* **2006**, *18*, 4875.
- (56) Smith, J. J.; Zharov, I. *Chem. Mater.* **2009**, *21*, 2013.
- (57) Yameen, B.; Kaltbeitzel, A.; Langner, A.; Muller, F.; Gosele, U.; Knoll, W.; Azzaroni, O. *Angew. Chem. Int. Ed.* **2009**, *48*, 3124.
- (58) Yameen, B.; Kaltbeitzel, A.; Langner, A.; Duran, H.; Muller, F.; G sele, U.; Azzaroni, O.; Knoll, W. *J. Am. Chem. Soc.* **2008**, *130*, 13140.
- (59) Yameen, B.; Kaltbeitzel, A.; Glasser, G.; Langner, A.; M ller, F.; G sele, U.; Knoll, W.; Azzaroni, O. *ACS Appl. Mater. Interfaces* **2010**, *2*, 279.
- (60) Friedman, R. M.; Hudis, J.; Perlman, M. L. *Phys. Rev. Lett.* **1972**, *29*, 692.
- (61) Suzuki, M.; Kishida, A.; Iwata, H.; Ikada, Y. *Macromolecules* **1986**, *19*, 1804.
- (62) Lovering, D. *NKD-6000 Technical Manual*; Aquila Instruments: Cambridge, U.K., 1998.
- (63) Zawodzinski, T. A. Jr.; Neeman, M.; Sillerud, L. O.; Gottesfeld, S. *J. Phys. Chem.* **1991**, *95*, 6040.
- (64) Rockland, L. B. *Anal. Chem.* **1960**, *32*, 1375.
- (65) Zhou, C.; Guerra, M. A.; Qiu, Z.-M.; Zawodzinski, T. A. Jr.; Schiraldi, D. A. *Macromolecules* **2007**, *40*, 8695.
- (66) Liu, W.; Zuckerbroel, D. J. *Electrochem. Soc.* **2005**, *152*, A1165.
- (67) Borup, R.; Meyers, J.; Pivovar, B.; Kim, Y. S.; Mukundan, R.; Garland, N.; Myers, D.; Wilson, M.; Garzon, F.; Wood, D.; et al. *Chem. Rev.* **2007**, *107*, 3904.
- (68) Beamson, G.; Briggs, D. *High Resolution XPS of Organic Polymers*; Wiley: Chichester, U.K., 1992.
- (69) Holmes, S. A.; Thomas, T. D. *J. Am. Chem. Soc.* **1975**, *97*, 2337.
- (70) Yang, J. C.; Jablonsky, M. J.; Mays, J. W. *Polymer* **2002**, *43*, 5125.
- (71) Iddon, P. D.; Robinson, K. L.; Armes, S. P. *Polymer* **2004**, *45*, 759.
- (72) Kaka , S.; Pramuanjaroenkij, A.; Vasiliev, L. *Mini-Micro Fuel Cells: Fundamentals and Applications*; Springer: Dordrecht, The Netherlands, 2008.
- (73) Ward, L. J. *Patent No WO 03/101621*, 11th December 2003.
- (74) Guo, X.; Fang, J.; Watari, T.; Tanaka, K.; Kita, H.; Okamoto, K. *Macromolecules* **2002**, *35*, 6707.
- (75) Einsla, M. L.; Kim, Y. S.; Hawley, M.; Lee, H.-S.; McGrath, J. E.; Liu, B.; Guiver, M. D.; Pivovar, B. S. *Chem. Mater.* **2008**, *20*, 5636.
- (76) Parsons, A. F. *An Introduction to Free Radical Chemistry*; Blackwell Science Ltd: Oxford, U.K., 2000.
- (77) Mayo, F. R.; Lewis, F. M.; Walling, C. J. *Am. Chem. Soc.* **1948**, *70*, 1529.
- (78) Giese, B. *Angew. Chem., Int. Ed.* **1983**, *22*, 753.
- (79) Dippy, J. F. J. *Chem. Rev.* **1939**, *25*, 151.
- (80) Nozaki, K.; Sato, N.; Ikeda, K.; Takaya, H. *J. Org. Chem.* **1996**, *61*, 4516.

(81) Teare, D. O. H.; Schofield, W. C. E.; Roucoules, V.; Badyal, J. P. *S Langmuir* **2003**, *19*, 2398.

(82) ten Brink, G. J.; Arends, I. W. C. E.; Sheldon, R. A. *Science* **2000**, *287*, 1636.

(83) Berron, B. J.; Payne, P. A.; Jennings, G. K. *Ind. Eng. Chem. Res.* **2008**, *47*, 7707.